4 R. Mayer, G. Domschke, S. Bleisch, J. Fabian, A. Bartl and A. Stasko, *Coll. Czech. Chem. Commun.*, 1984, **49**, 684.

5 V. A. Bagryansky, I. V. Vlasyuk, Yu. V. Gatilov, A. Yu. Makarov, Yu. N. Molin, V. V. Shcherbukhin and A. V. Zibarev, *Mendeleev Commun.*, 2000, 5.

6 I. V. Vlasyuk, V. A. Bagryansky, N. P. Gritsan, Yu. N. Molin, A. Yu. Makarov, Yu. V. Gatilov, V. V. Shcherbukhin and A. V. Zibarev, *Phys. Chem. Chem. Phys.*, 2001, **3**, 409.

7 N. P. Gritsan, V. A. Bagryansky, I. V. Vlasyuk, Yu. N. Molin, M. S. Platz and A. V. Zibarev, *Izv. Akad. Nauk, Ser. Khim.*, 2001, 1973 (*Russ. Chem. Bull., Int. Ed.*, 2001, **50**, 2064).

8 K. V. Shuvaev, V. A. Bagryansky, N. P. Gritsan, A. Yu. Makarov, Yu. N. Molin and A. V. Zibarev, *Mendeleev Commun.*, 2003, 178.

9 R. T. Boere, K. H. Mock, S. Derrick, W. Hoogerdijk, K. Preuss, G. Yip and M. Parvez, *Can. J. Chem.*, 1993, **71**, 473.

10 A. N. Terenin, *Fotokhimiya krasitelei i rodstvennykh organicheskikh soedinenii* (*Photochemistry of Dyes and Related Organic Compounds*), AN SSSR, Moscow, 1947, pp. 128–129 (in Russian).

11 T. Maaninen, R. Laitinen and T. Chivers, *Chem. Commun.*, 2002, 1812.

12 H. W. Roesky, K. L. Weber, M. Noltemeyer and G. M. Sheldrick, *Z. Naturforsch. B*, 1984, **39**, 163.

13 I. Yu. Bagryanskaya, Yu. V. Gatilov, A. Yu. Makarov, A. M. Maksimov, A. O. Miller, M. M. Shakirov and A. V. Zibarev, *Heteroatom Chem.*, 1999, **10**, 113.

14 A. Yu. Makarov, I. Yu. Bagryanskaya, Yu. V. Gatilov, T. V. Mikhalina, M. M. Shakirov, L. N. Shchegoleva and A. V. Zibarev, *Heteroatom Chem.*, 2001, **12**, 563.

15 A. Yu. Makarov, I. Yu. Bagryanskaya, F. Blockhuys, C. Van Alsenoy, Yu. V. Gatilov, V. V. Knyazev, A. M. Maksimov, T. V. Mikhalina, V. E. Platonov, M. M. Shakirov and A. V. Zibarev, *Eur. J. Inorg. Chem.*, 2003, 77.

16 J. W. Bats, H. Fuess, K. L. Weber and H. W. Roesky, *Chem. Ber.*, 1983, **116**, 1751.

# Manganese complexes with aliphatic amines in aqueous solutions and in the solid state

Evgeni M. Glebov,*[a] Vjacheslav P. Grivin,[a] Victor F. Plyusnin,[a] Alexander V. Udal'tsov,[b] Zhang Yiheng,[c] Andreas Herrmann,[c] Gerd Kaupp[c] and Johannes G. Vos[d]

[a] Institute of Chemical Kinetics and Combustion, Siberian Branch of the Russian Academy of Sciences, 630090 Novosibirsk, Russian Federation. Fax: +7 3832 34 2350; e-mail: glebov@ns.kinetics.nsc.ru
[b] Institute of Biology, Komi Center, Urals Branch of the Russian Academy of Sciences, 167982 Syktyvkar, Russian Federation
[c] Organic Chemistry I, University of Oldenburg, D-26129 Oldenburg, Germany
[d] School of Chemical Sciences, Dublin City University, F-31062 Dublin, Ireland

The complexation of bivalent manganese with aliphatic amines in aqueous solutions and the composition of the precipitates obtained from the systems were studied.

In photosynthesis, solar energy is transformed into chemical products *via* carbon dioxide reduction. Simultaneously, water is oxidised at the reaction centre of Photosystem II (PSII).[1,2] This process occurs in the oxygen evolving complex (OEC) containing four manganese ions. Although the OEC structure has not been clearly identified, the modeling of water photodecomposition is the subject matter of intense investigation.[3–8]

One of the approaches to OEC modeling is based on the use of donor–acceptor complexes formed by solutes and water molecules.[9–11] The irradiation of solutions containing porphyrin associates and their donor–acceptor complexes with water gives rise to a proton release.[10] Water molecules are assumed to be the source of such protons. A system containing the assemblies of *meso*-tetra(*p*-aminophenyl)porphin (TAPP) and, probably, polynuclear manganese triethylamine (TEA) complexes has been studied.[11] These water-containing assemblies display a photochemical activity, in which the photolysis products are subjected to protonation with protons most likely coming from these water molecules.[10,11] Thus, the combined manganese/porphyrin complex is a promising system for the photocatalytic splitting of water.

To determine the mechanism of operation of the model system of water photodecomposition[11] and to develop methods for its optimization, one should study in detail the system components including the associates and donor–acceptor complexes of porphyrins with water and manganese complexes with alkylamines. Whereas the porphyrin complexes have been studied,[9–11] the complexation of manganese ions and aliphatic amines is not clearly understood. As in the natural OEC, it is essential that the manganese complex involved in the model system is polynuclear. The interaction between $Mn^{II}$ ions and TEA in water solutions gives rise to a complex, which has no ESR spectrum and is likely to contain two or more manganese ions.[11] The
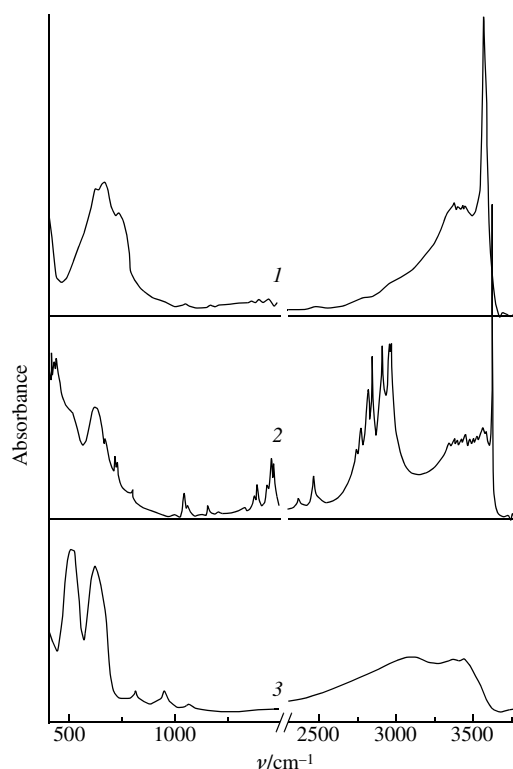


**Figure 1** IR spectra of precipitates obtained by the reaction between $MnCl_2$ and DEA in aqueous solutions. (*1*) 0.8 M $MnCl_2$ + 0.4 M DEA, (*2*) 0.8 M $MnCl_2$ + 2.4 M DEA and (*3*) 0.004 M $MnCl_2$ + 0.004 M DEA.
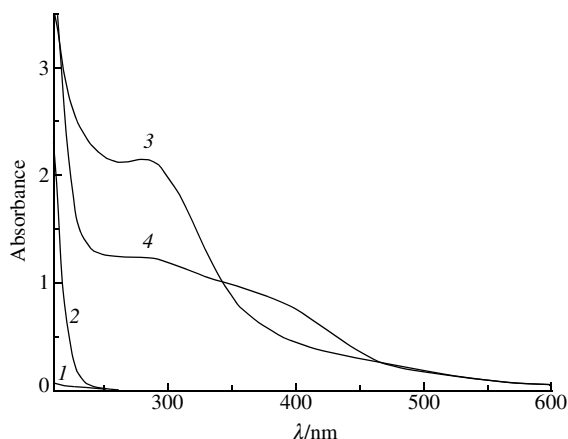
**Figure 2** Optical absorption spectra of manganese complexes with DEA in water solutions. (*1*) 0.001 M MnCl$_2$; (*2*) 0.02 M DEA; (*3*) the spectrum of solutions after the mixing of 0.001 M MnCl$_2$ with 0.02 M DEA after 145 h of storage in the dark (twofold dilution); (*4*) the spectrum of solution at initial concentrations of MnCl$_2$ and DEA of 2×10$^{-4}$ and 0.02 M, respectively, after 145 h of storage in the dark.

aim of this work was to study the properties of manganese complexes with diethylamine (DEA) and to compare the results with those found for the manganese/TEA compounds.

MnCl$_2$·4H$_2$O, DEA and TEA (Aldrich) were used in this work. The reaction products were investigated using IR, UV and ESR spectroscopy, Atomic Force Microscopy and Scanning Near-Field Optical Microscopy (AFM/SNOM).[12] In AFM, a solid surface is scanned under a constant van der Waals force acting on a tip in the range 10$^{-9}$–10$^{-7}$ N. The data extracted were used to construct a topographic image of the surface. In SNOM, the surface is scanned by a light beam spreading through an optical fiber. To obtain the SNOM image, the feedback signal is needed, which is usually an AFM signal. In this case, the optical fiber is used as an AFM tip in the shear force mode. The SNOM signal (488 nm) is an optical image. The reflection back to the fiber SNOM setup under the shear force AFM control was used.[12–14] The near-field reflected light in the shear force gap is strongly enhanced with respect to constant far-field stray light. The variations in near-field reflected light provide the SNOM image. Optical resolution was determined by the fiber aperture (10–30 nm).

Mixing the aqueous solutions of MnCl$_2$ and DEA causes the formation of precipitates, whose composition depends on the relative concentrations of reagents and dissolved oxygen. The ESR data indicated that, when the reagent concentrations substantially exceed that of oxygen, the white precipitate formed is a Mn$^{II}$ compound. Figure 1 shows the IR spectra of the precipitates. For excess manganese ions (Figure 1, curve *1*), the precipitate is assumed to be [Mn(ClOH)(H$_2$O)$_4$] (typical coordination number for Mn$^{II}$ complexes is 6[15]).

DEA constant of basicity is $K_B = 10^{-3}$ M.[16] The pH of the solution is 12.3 or 12.8 for [DEA] = 0.4 or 2.4 M, respectively. Under these conditions, MnCl$_2$ reacts with the hydroxide ion. The reaction runs under conditions of excess manganese ions (0.8 M) above the concentration of OH$^-$ (0.02–0.05 M). In this case, the precipitation of the [Mn(ClOH)(H$_2$O)$_4$] complex is proposed to occur, rather than the precipitation of Mn(OH)$_2$, as in the case of the reaction between Mn$^{2+}$ and alkalis. For excess amine (Figure 1, curve *2*), the precipitate is [Mn(OH)$_2$(H$_2$O)$_m$(Et$_2$NH)$_{4-m}$] (or [Mn(ClOH)(H$_2$O)$_m$(Et$_2$NH)$_{4-m}$], where $m = 1$–3).[17] With a deficiency of amine, no complexes are formed by Mn$^{II}$ ions with the amine in solution (based on UV and ESR spectra).

When reagent concentrations are comparable with those of water-dissolved oxygen, Mn$^{II}$ is oxidised. In this case, the precipitate becomes brown and contains (according to ESR data[17]) Mn$^{IV}$ compounds. The appearance of the precipitate and its IR spectrum (Figure 1, curve *3*) are consistent with the appearance and the spectrum of the precipitate resulting from the mixing of MnCl$_2$ and NaOH solutions under similar conditions. Most
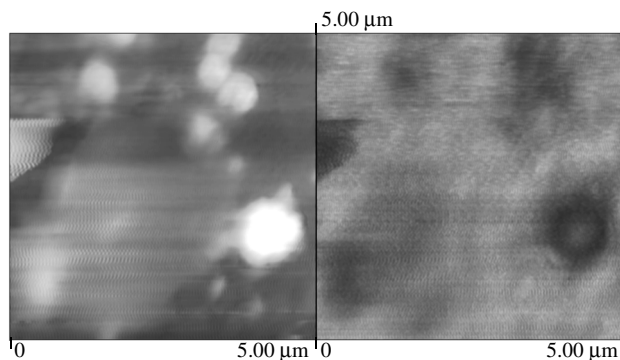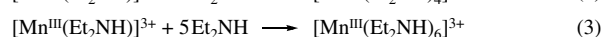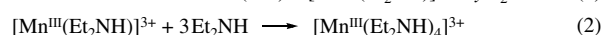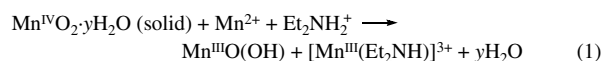


**Figure 3** AFM (to the left) and SNOM (to the right) images of samples prepared by the evaporation of water from the solution containing MnCl$_2$ and TEA (0.004 M, both). Substrate, mica plate. The near-field gain factor was 3–4.

likely, in both cases, the precipitate is the manganese oxide hydrate MnO$_2$·$y$H$_2$O.

For these low concentrations of Mn$^{II}$ and DEA, the dissolution of the initial precipitate is accompanied by the formation of complexes, the UV spectra of which are shown in Figure 2. In this case, the manganese ions display no ESR spectrum and likely occur in a trivalent state.[18] For the complex with an absorption band at 280 nm (Figure 2, curve *3*), the ratio between the numbers of ligands and metal ions (DEA/Mn) is 4, as determined by the Job's plot method.[19] Assuming that the total coordination number is 6,[15] possible structures for complexes with four DEA molecules and various sets of H$_2$O, OH$^-$, and Cl$^-$ ligands are, for example, [Mn(DEA)$_4$(H$_2$O)$_2$]$^{3+}$ or [Mn(DEA)$_4$(OH)$_2$]$^+$. For higher DEA/Mn ratios, the formation of another complex with an absorption band at 380–390 nm (Figure 2, curve *4*) was observed. In this case, the DEA/Mn ratio determined for the complex absorbing at 380 nm by the method of molar ratios[19] is 6.

The Mn$^{III}$ complex formation was probably due to dissolution of the precipitate containing Mn$^{IV}$ and caused by a comproportionation reaction between Mn$^{IV}$ in the solid phase and Mn$^{II}$ in solution. Possible pathways to the formation of these compounds are shown below (apart from Et$_2$NH, other ligands are present in the coordination sphere of the complexes, but they are omitted for clarity). The initial process (1) involves the protonated form of an amine.

$$Mn^{IV}O_2 \cdot yH_2O \text{ (solid)} + Mn^{2+} + Et_2NH_2^+ \longrightarrow$$
$$Mn^{III}O(OH) + [Mn^{III}(Et_2NH)]^{3+} + yH_2O \quad (1)$$

$$[Mn^{III}(Et_2NH)]^{3+} + 3Et_2NH \longrightarrow [Mn^{III}(Et_2NH)_4]^{3+} \quad (2)$$

$$[Mn^{III}(Et_2NH)]^{3+} + 5Et_2NH \longrightarrow [Mn^{III}(Et_2NH)_6]^{3+} \quad (3)$$

The mechanism proposed for the reaction between MnCl$_2$ and DEA does not predict the formation of polynuclear complexes of manganese (either of Mn$^{II}$ at high reagent concentrations or of Mn$^{III}$ and Mn$^{IV}$ at low reagent concentrations). However, multinuclear complexes of manganese were proposed[11] to occur in the reactions between MnCl$_2$ and TEA. One could, therefore, expect that the chemical composition of the solid sample prepared by solvent evaporation from a solution containing MnCl$_2$ and TEA would be less homogeneous than that of the sample prepared with the use of DEA. This assumption was investigated by experiments using the simultaneous recording of AFM and SNOM images[12–14] of corresponding samples. The samples were prepared at low reagent concentrations, which implies that dominating manganese species should be Mn$^{III}$/amine complexes.

Figures 3 and 4 show the AFM and SNOM images of samples obtained by evaporating the solvent from solutions that contain complexes of Mn$^{III}$ with TEA and DEA, respectively. The evaporation was performed by heating of a drop of the solution on the surface of mica at 40 °C. The AFM image is determined by the surface topography, and the SNOM image is determined by chemical composition.[12] To demonstrate the SNOM image, the surface must contain domains, which com-

5.00 μm

0              5.00 μm 0             5.00 μm
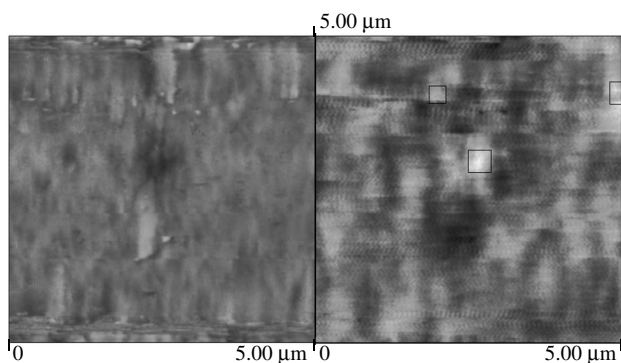
**Figure 4** AFM (to the left) and SNOM (to the right) images of samples prepared by the evaporation of water from the solution containing $MnCl_2$ and DEA (0.004 M, both). Substrate, mica plate. The near-field gain factor was 3–4. Boxes on the SNOM image mark the regions of bright contrast (see the text).

position is different from the composition of other surface. The typical size of these domains should be not less than the spatial resolution of the method (10–30 nm).[12,14] All the samples studied revealed local variations in domain composition in the SNOM images.

The correspondence between the topographic image and the contrast observed in SNOM indicates that relief inhomogeneity is due to the particles whose chemical nature differs from that of the basic substance. This holds for the samples prepared from a solution containing $MnCl_2$ and TEA (Figure 3). The SNOM image appears as a more or less negative image of the AFM one due to contrast of the features. In principle, the positive contrast is also possible; however, at present, the sign of the image cannot be predicted.[14] It is assumed that the basic sample surface is mainly created by a substance formed by water evaporation from the solutions containing the complexes $[Mn^{III}(Et_3N)_4]^{3+}$ and $[Mn^{III}(Et_3N)_6]^{3+}$ [similarly to the products of reactions (2) and (3) for DEA]. The proposed formula for this substance is $[MnCl_3(Et_3N)_3]$. The probable way of its formation is

$$[Mn^{III}(Et_3N)_4]^{3+} + 3Cl^- \longrightarrow [Mn^{III}(Et_3N)_3Cl_3] + Et_3N \qquad (4)$$
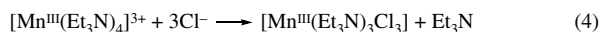
The regions of about 1 μm (Figure 3) are, probably, attributed to a substance produced by further clusterization of polynuclear manganese complexes. The substances, represented by these regions, probably, contain water molecules, which form a network of hydrogen bonds, and provide the stability of large clusters.

There is no full agreement between the topography and chemical contrast of the samples prepared from solutions containing $MnCl_2$ and DEA (Figure 4). The SNOM image is less homogeneous than the topographical one, and a typical size of its regions is 1 μm as well. Similarly to TEA, it is assumed that the bright regions of the SNOM image reflect the presence of mononuclear manganese complexes and the dark regions are attributed to the polynuclear complexes linked by water molecules. Polynuclear complexes (which are not present in the initial solution) are formed from the complexes $[Mn^{III}(Et_2NH)_4^{3+}L_1L_2]$ (possible $L_1$ and $L_2$ ligands are $H_2O$, $OH^-$ and $Cl^-$) and $[Mn^{III}(Et_2NH)_6]^{3+}$ upon water evaporation during the preparation of the samples.

The peculiarity of the SNOM image (Figure 4) is the presence of spots with very bright optical contrast. The coordinates of centres of these very bright spots (marked with boxes in the SNOM image, Figure 4) are, *e.g.*, (X = 2.6; Y = 2.9), (X = 2.0; Y = 4.0), (X = 4.9; Y = 4.1) (coordinates are measured in μm). The very bright spots are proposed to belong to the third species. It cannot be due to uncovered mica because the average roughness of the surface for these spots (determined from the AFM images) is not less than average for the whole sample. It could be proposed that high-reflecting areas belong to $MnCl_2$. Manganese(II) chloride could be formed during the evaporation of the solvent from solutions containing Mn(II) ions, which are partly present (in addition to $Mn^{III}$) in the initial mother liquor.[17]

The AFM/SNOM data indicate the tendency of the complexes of $Mn^{III}$ with amines to form polynuclear structures. For the Mn–TEA system, the polynuclear complexes are formed in the solid phase when both of the reagents are dissolved in water at an initial concentration of about 1 M.[11] For the Mn–DEA system, the formation of polynuclear complexes occurs only during the evaporation of the solvent from solutions containing $Mn^{III}$ complexes with DEA. Therefore, the tendency to form polynuclear complexes for the Mn–TEA system seems more pronounced than that for the Mn–DEA system. As a result, the $MnCl_2$ + TEA system is more promising for modeling the PSII OEC, as compared with the $MnCl_2$ + DEA system.

## References

1 V. K. Yachandra, K. Sauer and M. P. Klein, *Chem. Rev.*, 1996, **96**, 2927.
2 R. K. Clayton, *Photosynthesis*, Cambridge University Press, Cambridge, 1980.
3 L. Sun, H. Berglund, R. Dadydov, T. Norby, L. Hammarstrom, P. Korall, A. Borje, C. Philouze, K. Berg, A. Tran, M. Andersson, G. Stenhagen, J. Martenson, M. Almgren, S. Styring and B. Akermark, *J. Am. Chem. Soc.*, 1997, **119**, 6996.
4 W. Ruttinger and G. C. Dismukes, *Chem. Rev.*, 1997, **97**, 1.
5 V. L. Pecoraro, M. J. Baldwin and A. Gelasko, *Chem. Rev.*, 1994, **94**, 807.
6 J. Messinger, J. H. A. Nugent and M. C. W. Evans, *Biochemistry*, 1997, **36**, 11055.
7 H. Berglund-Baudin, L. Sun, R. Davydov, M. Sundahl, S. Styring, B. Akermark, M. Alngren and L. Hammarstrom, *J. Phys. Chem. A*, 1998, **102**, 2512.
8 L. Sun, L. Hammarstrom, B. Akermark and S. Styring, *Chem. Soc. Rev.*, 2001, **30**, 36.
9 A. V. Udal'tsov, *J. Photochem. Photobiol. B: Biol.*, 1997, **37**, 31.
10 A. V. Udal'tsov, *J. Photochem. Photobiol. A: Chem.*, 2000, **130**, 21.
11 A. V. Udal'tsov and Yu. V. Kovalev, *J. Photochem. Photobiol. A: Chem.*, 2000, **135**, 193.
12 G. Kaupp, in *Comprehensive Supramolecular Chemistry*, ed. J. E. D. Davies, Elsevier, Oxford, 1996, vol. 8, pp. 381–421.
13 G. Kaupp, A. Herrmann, J. Schmeyers and J. Boy, *J. Photochem. Photobiol. A: Chem.*, 2001, **139**, 93.
14 G. Kaupp, A. Herrmann and M. Haak, *J. Phys. Org. Chem.*, 1999, **12**, 797.
15 V. L. Pecoraro, *Photochem. Photobiol.*, 1988, **48**, 249.
16 A. M. Kim, *Organicheskaya khimiya* (*Organic Chemistry*), Izd-vo Novosibirskogo Universiteta, Novosibirsk, 2001, p. 679 (in Russian).
17 E. M. Glebov, V. P. Grivin, V. F. Plyusnin and A. V. Udal'tsov, *Izv. Akad. Nauk, Ser. Khim.*, 2005, in press.
18 P. Goldberg, J. Tesler, J. Krzystek, A. G. Montalban, L.-C. Brunel, A. G. M. Barrett and B. M. Hoffman, *J. Am. Chem. Soc.*, 1997, **119**, 8722.
19 M. T. Beck, *Chemistry of Complex Equilibria*, Van Nostrand Reinhold Company, London, New York, Toronto, Melbourne, 1970, pp. 100–120.